J. Biochem. **140**, 677–686 (2006)
doi:10.1093/jb/mvj195

Lipid Phosphate Phosphatases 1 and 3 Are Localized in Distinct Lipid Rafts

Masahiro Kai, Fumio Sakane, Yan-Jun Jia, Shin-ichi Imai, Satoshi Yasuda and Hideo Kanoh*

Department of Biochemistry, Sapporo Medical University School of Medicine, West-17, South-1, Sapporo 060-8556

Received August 23, 2006; accepted September 19, 2006

Lipid phosphate phosphatases (LPPs), integral membrane proteins with six transmembrane domains, dephosphorylate a variety of extracellular lipid phosphates. Although LPP3 is already known to bind to Triton X-100–insoluble rafts, we here report that LPP1 is also associated with lipid rafts distinct from those harboring LPP3. We found that LPP1 was Triton X-100–soluble, but CHAPS-insoluble in LNCaP cells endogenously expressing LPP1 and several LPP1 cDNA–transfected cells including NIH3T3 fibroblasts. In addition to the non–ionic detergent insolubility, LPP1 further possessed several properties formulated for raft-localizing proteins as follows: first, the CHAPS-insolubility was resistant to the actin-disrupting drug cytochalasin D; second, the CHAPS-insoluble LPP1 floated in an Optiprep density gradient; third, the CHAPS insolubility of LPP1 was lost by cholesterol depletion; and finally, the subcellular distribution pattern of LPP1 exclusively overlapped with that of a raft marker, cholera toxin B subunit. Interestingly, confocal microscopic analysis showed that LPP1 was distributed to membrane compartments distinct from those of LPP3. Analysis using various LPP1/LPP3 chimeras revealed that their first extracellular regions determine the different Triton X-100 solubilities. These results indicate that LPP1 and LPP3 are distributed in distinct lipid rafts that may provide unique microenvironments defining their non-redundant physiological functions.

Key words: lipid phosphate phosphatase, lipid rafts, microdomains, phosphatidic acid phosphatase, Triton X-100.

Abbreviations: LPP, lipid phosphate phosphatase; CHAPS, 3-[(3-cholamidopropyl)dimethylammonio]-1-propanesulphonate; PA, phosphatidic acid; MβCD, methyl-β-cyclodextrin; GFP, green fluorescent protein; CFP, cyan fluorescent protein; VSVG, vesicular stomatitis virus glycoprotein; CTxB, cholera toxin B subunit; PBS, phosphate-buffered saline.

Lipid phosphate phosphatases (LPPs) were initially cloned as the plasma membrane–bound (type 2) phosphatidic acid phosphatases (*1*, *2*), which convert phosphatidic acid (PA) to diacylglycerol (*3*). The enzymes, when assayed in vitro using Triton X-100 micelles of substrates, were subsequently shown to dephosphorylate a variety of lipid phosphates in addition to PA, including lyso-PA (*2*, *4*), sphingosine-1-phosphate (*2*, *4*), ceramide-1-phosphate (*2*, *4*), diacylglycerol pyrophosphate (*5*), and *N*-oleoyl ethanolamine phosphoric acid (*6*). The type 2 phosphatidic acid phosphatases were thus renamed as LPPs in view of the multifunctional catalytic properties (*7*). The substrates of LPPs are all known to act as signaling lipids, suggesting the importance of the enzymes in the control of a wide range of cellular functions. Indeed, the physiological importance of this class of enzymes has been shown by the function of *Drosophila* Wunen (8) and Wunen 2 (*9*), which regulate critically germ cell migration in the fly embryo. Moreover, the mouse embryos deficient in LPP3 failed to form extra-embryonic vasculature (*10*).

*To whom correspondence should be addressed. Tel: +81-11-611-2111, Fax: +81-11-622-1918, E-mail: kanoh@sapmed.ac.jp

So far, the two mammalian LPP isoforms, LPP1 and LPP3, have been best characterized. Like other members of the LPP family, both enzymes share basically the same structure, possessing six transmembrane regions (*7*, *11*, *12*) and being *N*-glycosylated at a single conserved site (*1*, *2*, *7*). Common to both LPPs, the amino acid residues essential for catalytic activity are well conserved among diverse family members and are located at the second and third extracellular regions, thus suggesting that LPPs are *ecto*-enzymes hydrolyzing extracellular lipid phosphates (*1*, *2*, *11–13*). Indeed, cell surface LPP activities have been demonstrated for LPP1 (*14*, *15*) and LPP3 (*16*) expressed in various cells. Overexpression of either LPP1 or LPP3 in ovarian cancer cell lines resulted in a decreased lyso-PA level in the culture medium and concomitantly in a suppressed cell growth, indicating that LPPs commonly attenuate extracellular growth signals (*17–19*). However, the physiological implications of LPP1 and LPP3 appeared to be distinct in different experiments. For example, the activation of mitogen activated protein kinase and DNA synthesis occurring in HEK293 cells could be attenuated by the expression of LPP1 but not of LPP3 (*20*). It should be noted here that the attenuation of cell growth could not be accounted for by the catalytic activity of LPP1 hydrolyzing extracellular lyso-PA (*20*, *21*). On the other

hand, LPP3 but not LPP1 has been reported to be capable of hydrolyzing PA generated by phospholipase D2 (*22*). The fact that LPP isoforms are not redundant functionally has also been shown in Drosophila, where mammalian LPP3 can participate in metabolizing germ cell–specific factors, whereas mammalian LPP1 fails to affect germ cell migration (*23*).

The mechanisms underlying non-redundant functions of different LPP isoforms as described above are worthy of further investigation. Such non-redundancy may, at least in part, arise from distinct localizations of LPPs in subcellular microdomains. The localization of LPP3 in TritonX-100–insoluble caveolae fraction has been implicated in the control of lipid signaling mediated by phospholipase D2 (*22*). In this case LPP1 was found Triton X-100–soluble, and the signaling function of this isoform remains unclear. It is also shown that significant LPP activities are present in caveolae-enriched fractions prepared from rat and mouse lung tissues (*24*). We also demonstrated that LPP1 and LPP3 are transported to the apical and basolateral subdomains, respectively, in polarized MDCK cells (*25*), where correct targeting of proteins to microdomains is often regulated through caveolae and non-caveolar raft fractions (*26*, *27*).

Lipid rafts are microdomains formed by the tight packing of sphingolipids and cholesterol in cell membranes (*27*). Evidence has been accumulated to show the function of rafts in the regulation of signal transduction (*28*) as well as membrane trafficking including exocytotic transport of raft-associated proteins (*26*). The regulation of functions of LPP isoforms via their raft association is an intriguing possibility. Recent work has shown that there are distinct types of rafts that can be distinguished with respect to localization patterns on the plasma membranes and different detergent-solubilities (*29*, *30*). These reports led us to reinvestigate the modes of raft association of LPP1 and LPP3 in detail. We found that LPP1 is also associated with rafts, which are segregated from those harboring LPP3, in a Triton-100–sensitive but CHAPS-resistant manner. Moreover, it was suggested that the first extracellular regions of the two LPP isoforms are responsible for their different raft localizations.

MATERIALS AND METHODS

Antibodies—Anti–human LPP1 antibody was raised in rabbits using a glutathione S-transferase–tagged C-terminal fragment (amino acids 250–284) (*2*) as an antigen. The anti-LPP1 antibody raised was affinity-purified using Sulfolink coupling gel (Pierce Biotechnology, Rockford, IL) linked to the antigen protein. Anti–glutathione S-transferase antibody contained in the anti-LPP1 antibody solution was absorbed by glutathione S-transferase–coupled gel (Pierce Biotechnology). This antibody did not react with human LPP3 (data not shown).

Other antibodies were purchased from the suppliers as follows: anti–green fluorescent protein (GFP) monoclonal antibody (Roche Molecular Biochemicals, Tokyo, Japan), anti-caveolin polyclonal antibodies (BD Biosciences-Transduction Laboratories, Lexington, KY), horseradish peroxidase–conjugated anti-mouse and anti–rabbit IgG antibodies (Jackson ImmunoResearch Laboratories, Inc., West Grove, PA), and anti-GFP polyclonal antiserum and Alexa594-conjugated anti–rabbit IgG antibody (Molecular Probes, Eugene, OR).

Plasmids Construction—The LPP1 and LPP3 proteins were C-terminally fused with either GFP (*2*) or cyan fluorescent protein (CFP) by cloning into the pEGFP-N3 or pECFP-N1 vectors (Takara Bio-Clontech, Tokyo, Japan). As described previously (*25*), LPP1/LPP3 chimeras were generated by sequential PCR using LPP1/pEGFP-N3 and LPP3/pEGFP-N3 as templates. In this case, parts of the LPP1 coding sequence were replaced with the corresponding regions of LPP3 according to the sequence alignments described previously (*2*). The sequences comprising LPP1/LPP3 chimeras are as follows (the numbers represent the amino acid residues of LPP1 and LPP3): LPP 1(1–86)/3(116–311), coding nucleotides (nt) 1–258 of LPP 1 and nt 346–933 of LPP 3; LPP 1(1–13)/3(41–311), nt 1–39 of LPP 1 and nt 121–933 of LPP 3; LPP3/1(14–29)/3(58–311), nt 40–87 of LPP1 and nt 1–120 and 172–933 of LPP3; LPP3(1–57)/1(30–57)/3(83–311), nt 88–171 of LPP1 and nt 1–171 and 249–933 of LPP3. All point mutations were achieved using Quick-Change Site-directed Mutagenesis Kit (Stratagene, La Jolla, CA), and were verified by sequencing. Two clones from separate mutagenesis reactions were selected and transfected separately to confirm the authenticity of the reaction products.

Cell Culture and Transfection—NIH3T3 and COS-7 cells were cultured in Dulbecco's modified Eagle's minimum essential medium (Sigma-Aldrich, Tokyo, Japan) supplemented with non-essential amino acids and 10% fetal bovine serum (Invitrogen, Tokyo, Japan). PC-12 cells were maintained in the same medium as above except for the supplement of 5% fetal bovine serum and 10% horse serum (Invitrogen). A human prostatic adenocarcinoma cell line LNCaP (ATCC, CRL-1740) was maintained in RPMI1640 medium supplemented with 10% fetal bovine serum from which lipids were depleted by the treatment with charcoal. To induce LPP1 expression, 10 nM R1881 (methyltrienolone, Dupont) was added into the medium and incubated for 48 h (*31*).

Preparation and polarization of MDCK cells stably expressing LPP1-GFP and LPP3-GFP were performed as described previously (*25*). To generate NIH3T3 cells stably expressing LPP1-CFP or LPP3-CFP, we used a retrovirus vector, pCX4bsr, a modified version of pCXbsr (*32*) lacking the internal initiation codons within gag region (a kind gift from Dr. T. Akagi, Osaka Bioscience Institute). Both the *Nhe*I restricted pCX4bsr encoding LPP1-CFP or LPP3-CFP fragment and the *Bam*HI-restricted vector were polished, and subsequently digested with *Not*I. Both fragments were ligated and the resulting LPP1-CFP/pCX4bsr or LPP3-CFP/pCX4bsr was used for retroviral infection essentially as described (*32*). Cells stably expressing either LPP1-CFP or LPP3-CFP were selected with Blasticidin S (10 μg/ml).

Transient transfection was achieved with LipofectAMINE Plus kit (Invitrogen). After transfection of the plasmids expressing LPP1, the cells were cultured for 24–36 h before use. Cholesterol depletion was accomplished by agitation of dishes with serum-free medium containing 10 mM methyl-β-cyclodextrin (MβCD, Sigma-Aldrich, Tokyo, Japan) at 37°C for 30 min before cell lysis. In the case of disruption of the cytoskeleton, the cells were incubated for 5 h at 37°C in the presence of 1 mM cytochalasin D (Sigma-Aldrich) prior to cell lysis. The cells

expressing the tsO45 strain of vesicular stomatitis virus glycoprotein (VSVG) were cultured for 24 h after transfection, and followed by a 6 h incubation at 32°C in the medium containing 1 μg/ml puromycin. The expression plasmid of the tsO45 strain of VSVG fused with CFP was constructed as described previously (*33*).

Detergent Lysis and Fractionation—Cells (12-well plate) expressing GFP-fused LPPs or VSVG were lysed for 30 min on ice in 100 μl of ice-cold lysis buffer (25 mM Tris-HCl, pH 7.4, 150 mM NaCl, 5 mM EDTA, 1 mM DTT, 5 μg/ml pepstatin, 5 μg/ml leupeptin, 1 mM phenylmethanesulfonyl fluoride) containing 10% sucrose and one of the following detergents: 1% Triton X-100, 1% octyl-β-D-glucoside and 20 mM CHAPS. Cell lysates were centrifuged at 100,000 × *g* for 1 h at 4°C. The supernatant and pellet were analyzed by SDS-PAGE followed by immunoblotting.

Optiprep Gradient Centrifugation—All subsequent procedures were done at 4°C. The NIH3T3 cells (35-mm dish) expressing GFP-fused LPPs were washed once and scraped in phosphate-buffered saline (PBS), and spun down at 350 × *g*. The cells were suspended and lysed in 200 μl of the lysis buffer containing 10% sucrose and either 1% Triton X-100 or 20 mM CHAPS. The lysates were suspended thoroughly by pipetting through a 200-μl yellow pipetting tip and incubated for 30 min on ice. Subsequently, 400 μl of 60% Optiprep (Nycomed Pharma AS, Asker, Norway) was added to the lysates and mixed gently, and the lysates were transferred to TLS55 centrifuge tubes (Beckman Coulter, Brea, CA). The samples were overlaid with 30%, 20%, 5% (600 μl, 600 μl, 200 μl, respectively) Optiprep dissolved in the lysis buffer containing 10% sucrose and either 1% Triton X-100 or 20 mM CHAPS. The gradients were spun at 130,000 × *g* for 4 h using a TLS55 rotor. After 10 fractions from the top of the gradient were collected, proteins present in these fractions were analyzed by immunoblotting.

Fluorescence Microscopy—NIH3T3 cells stably expressing either LPP1-CFP or LPP3-CFP were grown on poly-L-lysine–coated glass coverslips, and incubated with 2 μg/ml Alexa 594–conjugated cholera toxin B subunit (CTxB, Molecular Probe) for 1 h. After washing with PBS containing 1% BSA three times, cells were fixed with 3.7% formaldehyde and rinsed with PBS–1% BSA. Coverslips were mounted using Vectashield (Vector Laboratories, Burlingame, CA). Cells were examined using an inverted confocal laser scanning microscope (Zeiss LSM 510). In another experiment, NIH3T3 cells grown on poly-L-lysine–coated glass coverslips were transiently transfected with either LPP1/pEGFP-N3 or LPP3/pEGFP-N3. After 24 h, cells were fixed with 3.7% formaldehyde, permeabilized in PBS containing 0.1% Triton X-100, and blocked with PBS-1% BSA. Coverslips were then incubated with anti–caveolin-1 polyclonal antibody followed by incubation with Alexa 594–conjugated anti–rabbit IgG antibody. Fluorescence microscopy was performed as described above.

Immunoblotting—Immunoblot analysis of proteins was performed as described previously (*16*, *25*). The intensities of the bands on the immunoblot were quantified with the NIH-Image program (version 1.62).

Metabolic Labeling Experiments—NIH3T3 cells stably expressing LPP1-CFP (12-well plate) were incubated for 1 h in methionine- and cysteine-free DMEM and subsequently pulsed for 15 min with 150 μCi/ml ^{35}S-methionine/cysteine (Express Protein Labeling Mix; DuPont NEN, Boston, MA). Cells were then washed in PBS and chased in complete medium supplemented with 5 mM methionine and 2.5 mM cysteine. After the chase, the cells were washed with ice-cold PBS and lysed by the addition of the lysis buffer containing 10% sucrose and either 1% Triton X-100 or 20 mM CHAPS (200 μl). The lysates were incubated on ice for 30 min and fractionated into soluble and insoluble materials by a 30-min centrifugation at 100,000 × *g*. After the resulting pellets were resuspended in 200 μl of the lysis buffer, 10 μl of 20% octylglucoside was added into both the soluble and insoluble fractions. LPP1-CFP was isolated from the fractions by immunoprecipitation as described previously (*2*). Briefly, the fractionated samples were pretreated for 20 min on ice with 10 μl of 20% (w/v) formalin-fixed Staphylococcus aureus (Sigma-Aldrich) and were subsequently centrifuged for 5 min at 12,000 × *g*. The supernatants were incubated for 60 min on ice with 1 μl of anti-GFP polyclonal antiserum followed by the addition of 10 μl of 20% (w/v) Staphylococcus aureus and incubation for 30 min on ice. The immunoprecipitates were rinsed sequentially by the first wash buffer (25 mM Tris-HCl, pH 7.4, 0.6 M KCl and either 1% Triton X-100 or 20 mM CHAPS) and the second wash buffer (25 mM Tris-HCl, pH 7.4, and either 0.1% Triton X-100 or 2 mM CHAPS), and resolved by SDS-PAGE. The radioactive bands were visualized by a BAS2000 image analyzer (Fuji Film Co., Ltd., Tokyo, Japan).

RESULTS

LPP1 Is Soluble in Triton X-100 but Insoluble in CHAPS—We first determined whether LPP1 is associated with the cholesterol-sphingolipid rafts that are recovered as detergent-insoluble complexes upon solubilization of cells in Triton X-100 at low temperature (*27*, *28*). To this end, we expressed LPP1 that was C-terminally fused with GFP in NIH3T3 fibroblasts. LPP3-GFP, which was already reported to be distributed to Triton X-100–insoluble rafts (*22*), was also examined as a positive control. In immunoblot analysis of both LPPs, several bands were detected (Fig. 1A). As shown previously (*25*), the diffuse 62–67-kDa bands should correspond to the mature forms fully glycosylated, whereas the 55- and 56-kDa bands were immature species which were not fully modified. When the detergent insolubilities of the LPP isoforms were investigated, we quantified only the mature forms, because immature species of the enzymes are suggested to be localized in pre-Golgi organelle (*34*) and, thereby, unable to be incorporated into rafts, which are organized in the Golgi complex in mammalian cells (*35*). To begin with, NIH3T3 cells expressing either LPP1-GFP or LPP3-GFP were lysed in 1% Triton X-100 at 4°C, and the lysates were separated into supernatant (soluble) and pellet (insoluble) fractions by centrifugation at 100,000 × *g* for 1 h. Consistent with the earlier report (*22*), immunoblot analysis showed that the mature form of LPP3 was almost completely recovered in the Triton X-100–insoluble fraction, whereas most of LPP1 was Triton X-100–soluble (Fig. 1A). Quantification of the band intensities revealed that 97.0% ± 3.4 (n = 8) of LPP3 and 3.6% ± 3.0 (n = 7) of LPP1 were sedimented (Fig. 1B).

As controls, Triton X-100 solubilities of two plasma membrane–localized proteins, caveolin-1 and VSVG, were analyzed. We verified that caveolin-1, which is known to be associated with Triton X-100–insoluble rafts (*36*, *37*), was indeed shown to be Triton X-100–insoluble, whereas VSVG, a non-raft protein, was Triton X-100–soluble (Fig. 1, A and B).

Although the insolubility of a membrane protein in Triton X-100 is consistent with its being associated with cholesterol-sphingolipid raft, a complete solubility in Triton X-100 does not exclude the possibility that it still engages in other, albeit Triton X-100–sensitive, raft interactions. We thus determined whether the use of other detergents for solubilization might reveal such possible interactions involving LPP1. In the next experiment, NIH3T3 cells expressing LPP1 were lysed at 4°C with 20 mM CHAPS, another non-ionic detergent, and fractionated into supernatant and pellet. Upon centrifugation at 100,000 × *g* for 1 h, 95.0% ± 4.8 (n = 4) of LPP1 was sedimented in marked contrast with the result with Triton X-100 (Fig. 1, A and B). Caveolin-1 and LPP3 also showed an exclusive recovery in the pellets. Cell lysis with 1% octylglucoside, which disrupts all raft compartments (*38*), led to a complete solubilization of LPP1 as well as LPP3 and caveolin-1 (Fig. 1, A and B). VSVG was exclusively recovered in the supernatant after CHAPS treatment, excluding the possibility that LPP1 was non-specifically associated with the CHAPS-insoluble complexes.

To determine whether the CHAPS insolubility and Triton X-100 solubility of LPP1 are observed also in other cell types, we assayed the insolubilities to these detergents using COS-7 and PC-12 cells transiently expressing LPP1, and NIH3T3 and polarized MDCK cells stably expressing this isoform. In all cell-lines examined, LPP1 was soluble in Triton X-100 but insoluble in CHAPS (Fig. 1C) in consistent with the results obtained with NIH3T3 cells transiently expressing this isoform (Fig. 1, A and B). On the other hand, we confirmed that LPP3 was Triton X-100/CHAPS–insoluble in all cell lines examined.

To detect endogenous LPP1, we prepared anti-LPP1 antibody. The antibody specifically detected LPP1, but not LPP3, as assessed by immunoblot analysis (data not shown). Moreover, the expression of LPP1 was highly induced in LNCaP cells treated with androgen as reported previously (*31*). As shown in Fig. 1D, we confirmed that

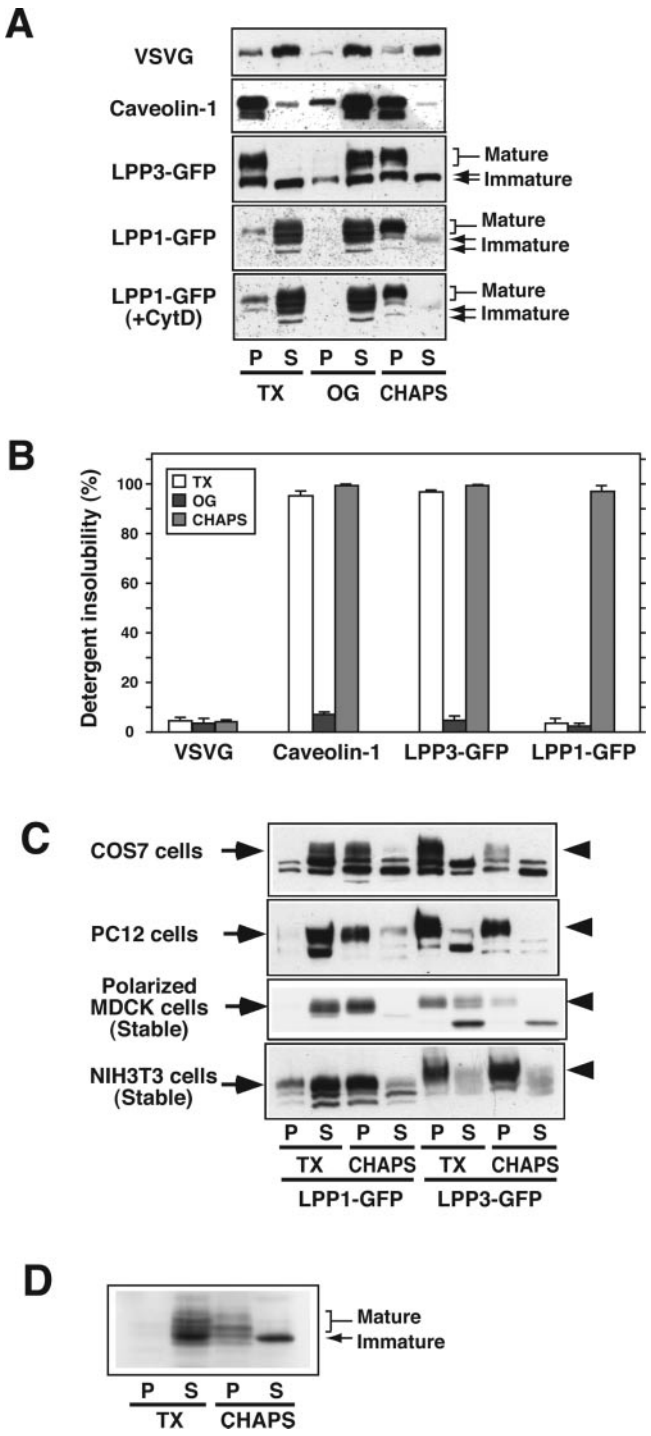

Fig. 1. **Analysis of detergent solubilities of LPPs.** (A) NIH3T3 cells transiently expressing VSVG-CFP (VSVG), LPP1-GFP or LPP3-GFP were lysed at 4°C in the presence of either 1% Triton X-100 (TX), 1% octylglucoside (OG) or 20 mM CHAPS. In several experiments, the cells were pretreated with 1 mM cytochalasin D (CytD) before lysis. After centrifugation at 100,000 × *g*, the entire supernatants (S) and pellets (P) were analyzed by immunoblotting. Transiently expressed proteins (VSVG-CFP, LPP1-GFP and LPP3-GFP) and endogenous caveolin-1 were detected with anti-GFP and anti-caveolin antibodies, respectively. The positions of mature and immature forms of LPPs are indicated at the right of each panel. (B) The band intensities were quantified. The protein recovered in pellets is shown as the percentage of total (supernatants plus pellets) and designated as detergent insolubility. In quantification of LPPs, only the bands of mature species were evaluated. Results are means ± SD (n = 3–8). (C) LPP1-GFP and LPP3-GFP were transiently expressed in COS7 and PC12 cells, and LPP1-CFP and LPP3-CFP were stably expressed in NIH3T3 and polarized MDCK cells. Fractionation was performed as described above, and the insolubilities of LPPs against Triton X-100 (TX) and CHAPS were analyzed. The positions of mature forms of LPP1 (arrows) and LPP3 (arrow heads) are indicated at the left and right of each panel, respectively. (D) LNCaP cells were incubated with R1881 for 48 h. Fractionation was performed as described above. The insolubilities of endogenous LPP1 against the indicated detergents were analyzed by immunoblotting using anti-LPP1 antibody. Representative results of two independent experiments are shown. The positions of mature and immature forms of LPP1 are indicated at the right of the blot.

endogenous LPP1 is soluble in Triton X-100 but insoluble in CHAPS. Taken together, these results indicate that the spectrum of detergent solubilities of LPP1 reflects its intrinsic properties. The finding of the insolubility of LPP1 in the non-ionic detergent described above suggests that LPP1 is a lipid raft-associating protein.

Insolubility of LPP1 in CHAPS Is Not Due to Interaction with Cytoskeletal Elements—Insolubility of a membrane protein in detergents such as CHAPS can be due to its association with detergent-resistant lipid rafts and/or its anchoring to cytoskeletal elements. Octylglucoside is a mild detergent that is thought to preserve the cytoskeleton and its associated proteins (*38*). Hence, the lack of sedimentation of LPP1 in octylglucoside (Fig. 1, A and B) suggests that the enzyme is not tightly associated with the cytoskeleton. This in turn suggests that the insolubility of this isoform in CHAPS is not due to cytoskeletal interactions. To investigate this directly, NIH3T3 cells expressing LPP1-GFP were pretreated with the actin-disrupting drug cytochalasin D (*39*) before lysis in CHAPS. As expected, this treatment did not affect the CHAPS insolubility of LPP1 (Fig. 1A). These observations confirm that the insolubility of LPP1 in CHAPS is not due to interaction with cytoskeletal elements.

Insolubility of LPP1 in CHAPS Reflects Its Association with Detergent-Resistant, Floating Complexes—Membrane proteins associated with the Triton X-100–insoluble lipid raft float in a sucrose or Optiprep density gradient (*27*, *28*). If LPP1 is associated with a CHAPS-insoluble lipid raft, this isoform should also float in the Optiprep density gradient. NIH3T3 cells expressing either LPP1-GFP or LPP3-GFP were lysed with 20mM CHAPS or 1% Triton X-100 at 4°C. Indeed, when CHAPS lysates of LPP1-transfected NIH3T3 cells were analyzed using a floatation equilibrium Optiprep density gradient, 81% of the mature form of LPP1 floated to the low-density buoyant fractions (Fig. 2A, top panel, lanes 1–3). LPP3 was also mainly recovered in the low-density fractions (72% of total, Fig. 2A, lower middle panel, lanes 1–3). On the other hand, when the cells were lysed with Triton X-100, consistent with the earlier report (*22*), 75% of LPP3 was floated to the low-density fractions. However, no LPP1 was found to float to fractions 1–3 when cells were lysed in Triton X-100 (Fig. 2B, top panel, lanes 1–3), in line with the complete solubility of this isoform in this detergent (Fig. 1).

The CHAPS-Resistant Floating Complexes Containing LPP1 Are Sensitive to Cholesterol Depletion—Given that cholesterol is enriched in the low-density fractions of the gradient containing the CHAPS-insoluble LPP1 complex, the question arises whether cholesterol is needed to maintain its structure, as is the case for Triton X-100–insoluble raft (*27*, *28*). To remove cholesterol from the plasma membrane, LPP1-transfected NIH3T3 cells were treated with MβCD, which is known to selectively deplete cholesterol from the plasma membrane (*40*). Moreover, the depletion of plasma membrane cholesterol is known to destabilize the raft compartment and to decrease raft-associated proteins in floating fractions on density gradient centrifugation (*41*). Upon cell treatment with 10 mM MβCD, cellular cholesterol was reduced to 7.6% of control as assessed by measuring the amount of ^{3}H-cholesterol, which was incorporated for a short time (15 min) into cellular membranes (thus, presumably mainly the plasma membrane) (data not shown). As shown in Fig. 2A (upper middle panel, lanes 1–3), when the cells were pretreated with 10 mM MβCD, the percentage of the mature LPP1 recovered in the low-density fractions was decreased from 81 to 14. Under the same conditions, the percentage of floating LPP3 was reduced from 72 to 24 (Fig. 2A, bottom panel, lanes 1–3). These results further indicate that LPP1 is associated with CHAPS-insoluble lipid rafts.

LPP1 Is Exclusively Colocalized with a Raft Marker, CTxB—To obtain further support for the lipid raft association of LPP1, we compared the intracellular localization of LPP1 with that of a raft marker CTxB, which specifically binds to the raft-associated lipid, ganglioside GM1 (*42*).

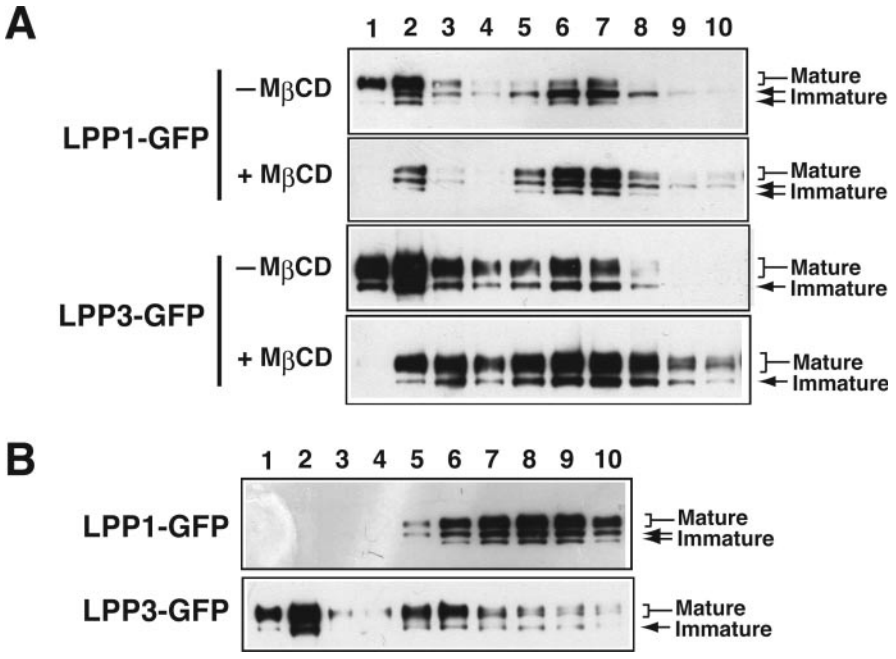

Fig. 2. **Optiprep density gradient analysis of LPP isoforms expressed in NIH3T3 cells.** NIH3T3 cells were transfected transiently with cDNAs encoding either LPP1-GFP or LPP3-GFP and lysed at 4°C in either 20 mM CHAPS (A) or 1% Triton X-100 (B). In some experiments using CHAPS, the cells were pretreated with 10 mM MβCD for 30 min before lysis. The cell lysates were subjected to flotation analysis on an Optiprep density step gradient, and the gradient fractions were analyzed by immunoblotting using anti-GFP antibody. The Optiprep concentration of the fractions 1, 2–4, 5–7 and 8–10 were estimated at 5, 20, 30 and 40%, respectively. Representative results of at least three independent experiments are shown. The positions of mature and immature forms of LPPs are indicated at the right of each panel.

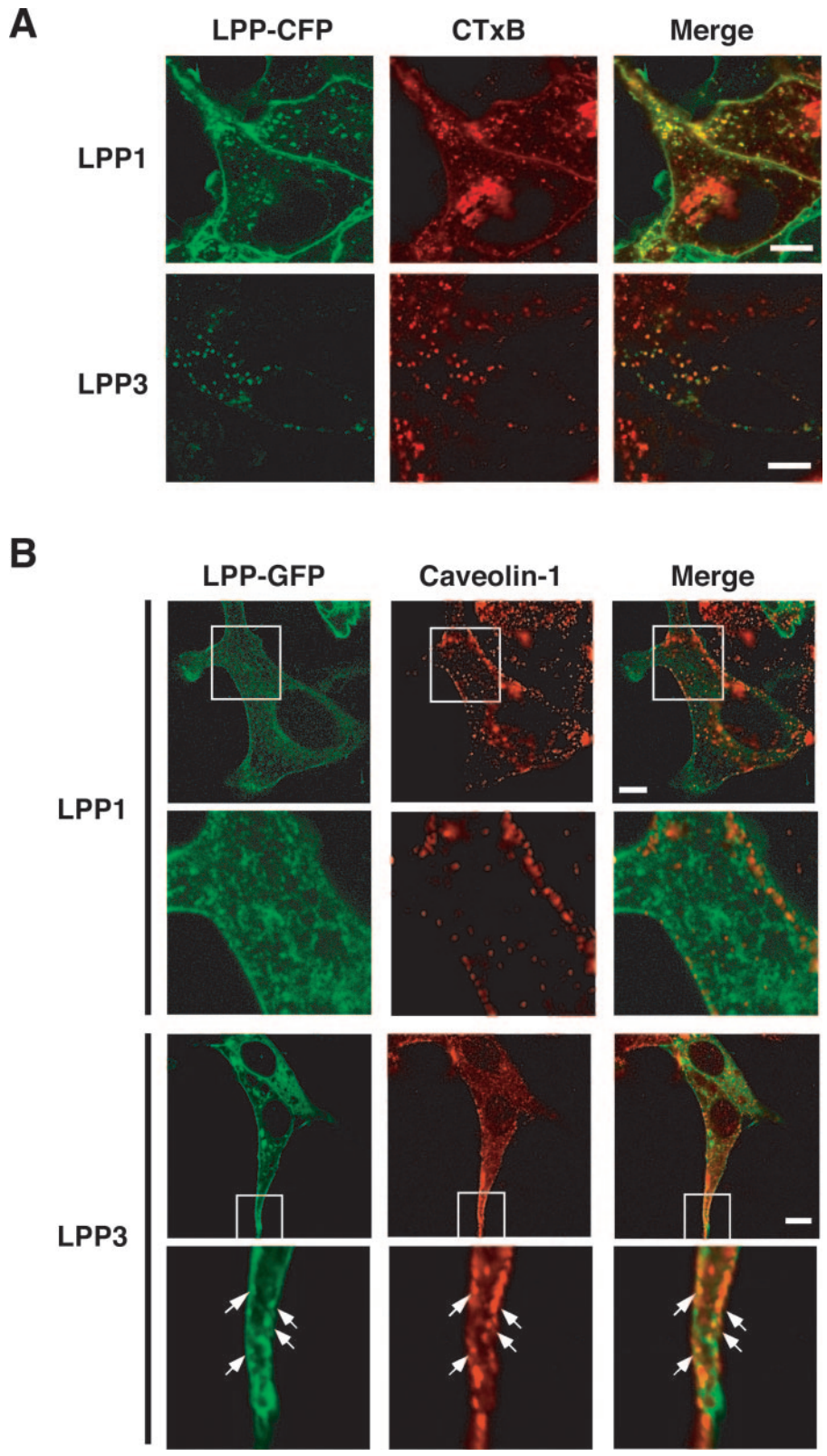

Fig. 3. **Intracellular localization of LPPs in NIH3T3 cells.** (A) NIH3T3 cells stably expressing either LPP1-CFP or LPP3-CFP were incubated with Alexa594-CTxB for 1 h. Cells were fixed and analyzed using a confocal laser scanning microscope as described in "MATERIALS AND METHODS." (B) NIH3T3 cells were transfected with cDNAs encoding LPP1-GFP or LPP3-GFP. After 24 h, endogenous caveolin-1 was immunostained using anti–caveolin-1 antibody, and analyzed as described above. In both sets of panels of LPP1 and LPP3, lower images are enlargements of the areas boxed in upper images. Several regions show an extensive signal overlap (arrows). The bar represents 10 μm. Representative results of at least three independent experiments are shown.

Fluorescence microscopy demonstrated that LPP1-CFP expressed in NIH3T3 cells was localized in the plasma membrane and intracellular vesicles (Fig. 3A). Interestingly, this distribution pattern of LPP1-CFP was exclusively overlapped with that of CTxB. LPP3 as a positive control was also distributed to the plasma membrane and intracellular vesicles, considerably coinciding with the localization pattern of CTxB. These results further support that LPP1 is associated with GM1-enriched microdomains (lipid rafts). Taken together, we

conclude that LPP1 is associated with CHAPS-insoluble lipid rafts.

LPP1 Is Associated with Lipid Raft Microdomains Segregated from Those Harboring LPP3—In the present study, we demonstrated that LPP1 and LPP3 displayed the different Triton X-100 solubilities, although both LPPs were associated with lipid rafts. Like the similar cases already reported (*30*, *40*), the discrepancy could be due to the association of LPP1 and LPP3 with distinct rafts. Thus, we compared the intracellular localization of LPP1 with that of caveolin-1, which was reported to be associated with LPP3-containing rafts (*22*), as internal reference. When LPP1-GFP or LPP3-GFP was expressed in NIH3T3 cells, both LPPs were distributed to the plasma membrane and the cytoplasm with a punctate pattern (Fig. 3B). However, although LPP3 was considerably colocalized with caveolin-1, we did not detect appreciable colocalization of LPP1 with caveolin-1. Together with the different Triton X-100 solubilities, the fluorescence microscopy data suggest that LPP1 and LPP3 are associated with distinct lipid rafts.

The CHAPS-Resistant Complexes Containing LPP1 Are Assembled in the Golgi Apparatus—We next attempted to characterize the properties of lipid raft association of LPP1. We previously reported that when the oligosaccharide of mature LPP1 was digested to a high mannose-type oligosaccharide by treatment with endo-β-galactosidase, its size reduced from 45 kDa to 41 kDa, concluding that a 41-kDa immature LPP1 was converted to a 45-kDa mature form by processing its oligosaccharide in the Golgi apparatus (*2*). We determined whether the LPP1-containing CHAPS-insoluble complexes are formed in the Golgi apparatus or at the plasma membrane, by comparing the time courses of the oligosaccharide processing and the acquisition of CHAPS insolubility of LPP1. To this end, we subjected NIH3T3 cells stably expressing LPP1-CFP to ^{35}S-methionine/cysteine pulse-chase analysis. The cells were lysed after a 15-min pulse-labeling and subsequent chase for various periods. The lysis was achieved with either Triton X-100 or CHAPS, and the cell lysates were separated into supernatants and pellets by ultracentrifugation. LPP1-CFP was immunoprecipitated from the detergent-insoluble (subsequently solubilized with octylglucoside) and soluble fractions, and analyzed by SDS-PAGE/autoradiography. A mature form of LPP1 appeared at 60 min after the pulse (Fig. 4). When the cells were lysed with CHAPS, the mature form was exclusively recovered in insoluble fractions in contrast to the immature band, which was only detected in soluble fractions. On the other hand, we confirmed that, with Triton X-100, both mature and immature forms of LPP1 were solely detected in soluble fractions. Consequently, it is suggested that the CHAPS insolubility (CHAPS raft-association) of LPP1 was acquired immediately after or during the Golgi stage of maturation/transport processes, but not at the plasma membrane. In mammalian cells, proteins associated with Triton X-100 (*35*, *36*)–, Lubrol WX (*27*)– and CHAPS (*39*)-insoluble rafts obtain their detergent insolubilities in the Golgi compartments. The results obtained here (Fig. 4) do not conflict with these observations, further supporting the notion that LPP1 is associated with CHAPS-insoluble lipid rafts.

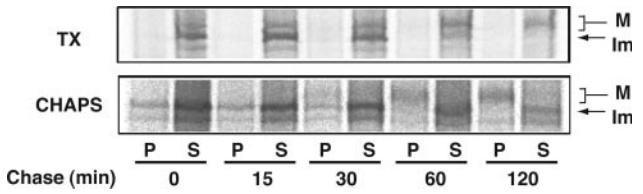

Fig. 4. **Time-dependent maturation and CHAPS-insolubility acquisition of LPP1.** NIH3T3 cells stably expressing LPP1-CFP were pulse-labeled with [^{35}S]methionine/cysteine for 15 min followed by chase for the indicated periods. Cells were lysed with 1% Triton X-100 (TX) or 20 mM CHAPS and fractionated by centrifugation at 100,000 × *g*. From the resulting supernatant (S) and pellets (P), which were resuspended with lysis buffer containing 1% octylglucoside, LPP1-CFP was immunoprecipitated using anti-GFP antibody. Immunoprecipitants were resolved by SDS-PAGE and radio-labeled proteins were detected using BAS2000. Mature (M) and immature (Im) forms of LPP1 are indicated at the right of each panel.

The First Extracellular Regions of LPPs 1 and 3 Determine Their Associations with Distinct Rafts—The findings that LPP isoforms showed distinct behaviors toward the Triton X-100 treatment prompted us to determine the regions of LPP1 and/or LPP3 responsible for their different solubilities. To this end, we prepared various LPP1/LPP3 chimeras (Fig. 5A), which were designed on the basis of the amino acids alignment as described previously (*2*), and tested their Triton X-100 solubilities. When NIH3T3 cells expressing LPP3-GFP and LPP1-GFP were lysed in Triton X-100, the percentages of the detergent-insoluble mature LPPs appeared to be 97 and 3.6, respectively (Fig. 5, A and B). When LPP1(1–86)/3(116–311), which consists of the N-terminal 86 amino acid residues of LPP1 and the C-terminal 187 amino acid residues of LPP3, was expressed in NIH3T3, we found that the Triton X-100 insolubility of the mutant was markedly decreased (from 97% of wild-type LPP3) to 18% (Fig. 5, A and B). This observation suggests that the solubility to Triton X-100 is determined by the N-terminal regions of LPP1 and/or LPP3 that consist of the first (N-terminal) intracellular, the first transmembrane and the first extracellular regions (see Fig. 5A). We next attempted to narrow down the responsible region. Replacement of the first intracellular [LPP1(1–13)/3(41–311)] and the first transmembrane [LPP3(1–40)/1(14–29)/3(58–311)] regions of LPP3 with the corresponding regions of LPP1 failed to affect the high Triton X-100 insolubility of LPP3 (Fig. 5, A and B). In contrast, LPP3(1–57)/1(30–57)/3(83–311) where the first extracellular region of LPP3 was replaced with the corresponding region of LPP1 exhibited a marked decrease of the detergent insolubility. We conversely prepared the LPP1(1–29)/3(58–82)/1(58–284) where the first extracellular region of LPP1 was replaced by the corresponding region of LPP3. For an unknown reason, however, this chimera expressed was localized in the endoplasmic reticulum but not at the plasma membrane, and no mature form was detected by immunoblot analysis (data not shown), thus hindering us from further investigation. From the results currently obtained, however, we conclude that the first extracellular regions of LPPs probably play essential roles in determining the extent of their Triton X-100 insolubilities.

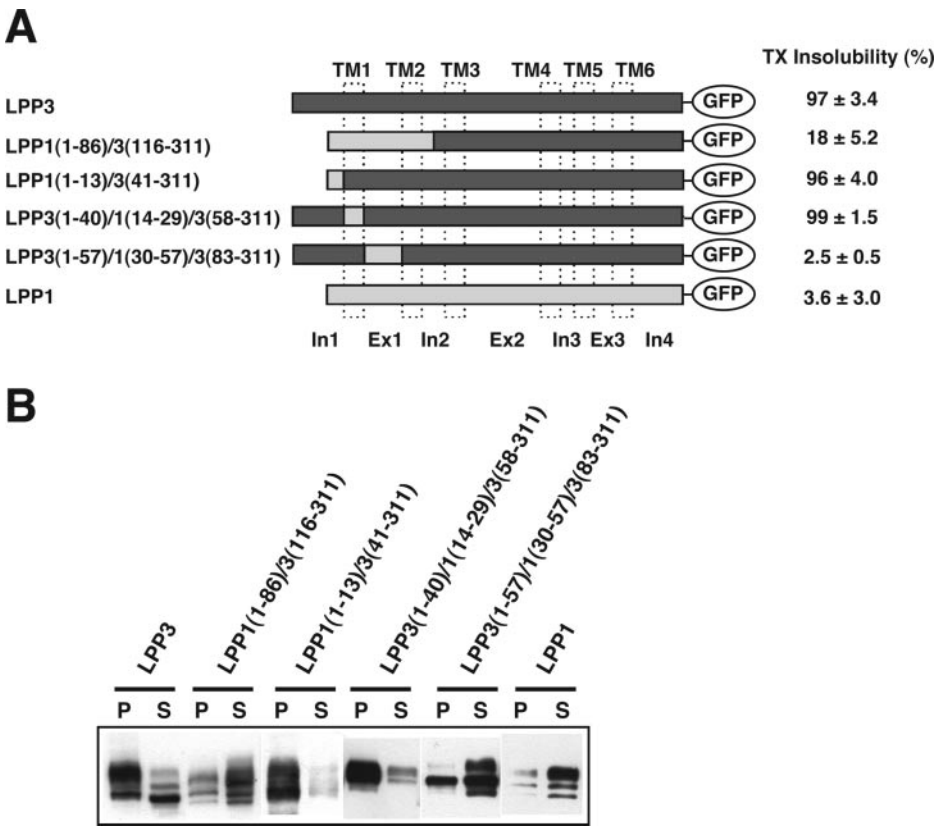

Fig. 5. **Triton X-100 solubilities of LPP1/LPP3 chimeras.** (A) Diagrammatic representation of LPP1, LPP3 and their chimera mutants. Chimeras are represented by a box with their N-termini to the left. The segments derived from LPP1 are shown as shaded boxes and those from LPP3 as black boxes. Boxes drawn by dotted lines indicate the positions of transmembrane domains (TM1–6). Four intracellular (In1–4) and three extracellular (Ex1–3) regions are shown at the bottom. From the results given in panel B, Triton X-100 (TX) insolubilities are determined as described in Fig. 1, in which results are shown as means ± SD (n = 3–4). (B) NIH3T3 cells transiently expressing LPP1, LPP3, or LPP chimera mutants were lysed at 4°C in 1% Triton X-100. After centrifugation at 100,000 × g, the supernatants (S) and pellets (P) were analyzed by immunoblotting using anti-GFP antibody.

DISCUSSION

Recent works have shown that different LPP isoforms have non-redundant functions (*20–22*). As a first step toward understanding the mechanisms underlying such non-redundancy, we previously demonstrated that LPP1 and LPP3 were transported to different subcellular domains (the apical and basolateral subdomains, respectively) in polarized MDCK cells (*25*). As a second step, in the present study, we attempted to gain more insight into the microdomain localization of LPP1 at the plasma membrane. The key observations made in this work are as follows: first, although LPP1 has been thought to be a non-raft-associated protein so far (*22*), this isoform was found to be associated with Triton X-100–soluble, but CHAPS-insoluble lipid rafts; secondly, LPP1 and LPP3 are distributed to rafts distinct from each other; and finally, the first extracellular regions of LPPs appear to be critical for determining their different raft localizations. The properties of lipid rafts harboring LPP1 and LPP3 are different from each other, at least, with respect to Triton X-100 solubility. Thus, it is tempting to speculate that the distinct lipid raft compartment may provide LPP1 with its own microenvironment defining its unique, non-redundant physiological function.

Sciorra and Morris (*22*) reported that when Triton X-100 lysates from HEK293 cells expressing LPP1 or LPP3 were fractionated on sucrose density gradients, only LPP3 was detected in the detergent-resistant membrane domain (lipid raft) fractions. They did not further characterize detergent solubilities of LPP1, and thus concluded that only LPP3 is associated with lipid rafts. In the present study, we analyzed the detergent solubilities of LPP1 in more detail. We found that LPP1 possesses five properties formulated for raft-associated proteins as follows: first, LPP1 was insoluble in non-ionic detergent CHAPS at low temperature (Fig. 1, A–D); second, the CHAPS-insolubility was resistant to the actin-disrupting drug cytochalasin D (Fig. 1A); third, the CHAPS-insoluble LPP1 was recovered in low-density buoyant membrane fractions (Fig. 2A); fourthly, the CHAPS insolubility was susceptible to cholesterol-depletion by MβCD, which disrupts raft structure (Fig. 2A); and finally, the intracellular distribution pattern of LPP1 exclusively overlapped with that of the lipid raft marker, CTxB (Fig. 3A). Moreover, the detergent insolubility of LPP1 was obtained immediately after or during the Golgi stage of maturation/transport processes but not at the plasma membrane (Fig. 4) in accordance with other lipid raft-associated proteins (*27*, *35*, *36*, *39*), further supporting the raft localization of LPP1.

Recently we reported that LPP1 and LPP3 were distributed to the apical and basolateral microdomains, respectively, in polarized MDCK cells (*25*). The idea that these different distribution patterns of the LPP isoforms are caused by their distinct raft associations as we demonstrated in the present study is very attractive. However, in polarized MDCK cells most Triton X-100–insoluble raft proteins are delivered to the apical membranes whereas Triton X-100–soluble proteins are localized in the basolateral membranes (*43*). Therefore, the raft distribution patterns in MDCK cells are not consistent with those of LPP isoforms as described in the present work. In addition,

we previously demonstrated the presence of the apical targeting signal of LPP1 and the basolateral targeting signal of LPP3 (*25*). When the N-terminal cytoplasmic region of LPP-3 was replaced with that of LPP1, which contained the apical targeting signal (see Fig. 5A), the Triton-insolubility of chimeric LPP3 remained unaffected. However, in the previous work (*25*), the microdomain distribution of the same chimeric LPP3 changed dramatically from the basolateral to the apical membranes. Although further work is needed to clarify such discrepant findings, we consider at the present stage that the microdomain localization of LPP isoforms can be dictated independently of their modes of raft localization.

LPP3, but not LPP1, was recently found to be involved in the homotypic cell–cell and cell–matrix interactions through its Arg-Gly-Asp cell adhesion sequence uniquely contained in the second extracellular region of this particular isoform (*44*). Moreover, we have already identified the apical and basolateral transport signals of LPP1 [FDKTRL present in the first (N-terminal) cytoplasmic region] and LPP3 (a dityrosine motif in the second cytoplasmic region), respectively (*25*). However, current knowledge of different properties of the isozymes derived from structural differences is still limited. In the present study, using a series of LPP1/LPP3 chimera proteins, we concluded that the first extracellular regions of LPPs are responsible for determining the extent of their Triton X-100 insolubilities (Fig. 5). The amino acid residues essential for catalytic activity are located in the second and third extracellular regions, and the Arg-Gly-Asp, cell adhesion, sequence of LPP3 exists in the second extracellular region. Therefore, we for the first time revealed a possible role of the first extracellular region. However, it is still unclear how the first extracellular region determines Triton X-100 insolubility (localization to different lipid rafts). A possible explanation of this finding is that although LPPs are basically CHAPS-insoluble, this region of LPP3 confers a Triton X-100 insolubility on this isozyme. Alternatively, it is possible to speculate that although LPPs are intrinsically insoluble to both of Triton X-100 and CHAPS, the region of LPP1 give it the Triton X-100 solubility. We cannot conclude which possibility is more likely at present. The sequence identity between the first extracellular regions of LPP1 and LPP3 (55%) is considerably lower than those of the second and third extracellular regions (70% and 86%, respectively) (*2*), which contain the catalytic sites (*11–13*). Thus, different amino acid residues between the first extracellular regions of the two isoforms may play an important role in gaining different Triton X-100 solubility. However, further studies are required to elucidate this issue and, moreover, to identify the putative raft-binding domain probably included in the first extracellular region(s).

LPP1a is an alternative splicing product from the gene encoding LPP1, and Gly-21–Val-70 in LPP1 is different from the corresponding region of LPP1a (*6*). Interestingly, because this region includes the first extracellular region of LPP1, it is probable that the Triton X-100 solubility of LPP1a is different from that of LPP1. Indeed, Nanjundan and Possmayer (*24*) revealed that, using pulmonary epithelial cells, LPP recovered in Triton X-100–insoluble raft fractions was LPP1 and/or LPP1a. In the present study, LPP1 was persistently Triton X-100–soluble in all cell lines examined (Fig. 1), suggesting that the Triton X-100–insoluble LPP reported by Nanjundan and Possmayer is LPP1a.

This works was supported in part by Grants-in-Aid from the Ministry of Education, Culture, Sports, Science and Technology of Japan.

REFERENCES

1. Kai, M., Wada, I., Imai, S., Sakane, F., and Kanoh, H. (1996) Identification and cDNA cloning of 35 kDa phosphatidic acid phosphatase (Type 2) bound to plasma membranes. *J. Biol. Chem.* **271**, 18931–18938
2. Kai, M., Wada, I., Imai, S., Sakane, F., and Kanoh, H. (1997) Cloning and characterization of two human isozymes of Mg^{2+}-independent phosphatidic acid phosphatase. *J. Biol. Chem.* **272**, 24572–24578
3. Smith, S.W., Weiss, S.B., and Kennedy, E.P. (1957) The enzymatic dephosphorylation of phosphatidic acids. *J. Biol. Chem.* **228**, 915–922
4. Waggoner, D.W., Gomez-Munoz, A., Dewald, J., and Brindley, D.N. (1996) Phosphatidate phosphohydrolase catalyzes the hydrolysis of ceramide 1-phosphate, lysophosphatidate, and sphingosine 1-phosphate. *J. Biol. Chem.* **271**, 16506–16509
5. Dillon, D.A., Chen, X., Zeimetz, G.M., Wu, W.I., Waggoner, D.W., Dewald, J., Brindley, D.N., and Carman, G.M. (1997) Mammalian Mg^{2+}-independent phosphatidate phosphatase (PAP2) displays diacylglycerol pyrophosphate phosphatase activity. *J. Biol. Chem.* **272**, 10361–10366
6. Hooks, S.B., Ragan, S.P., and Lynch, K.R. (1998) Identification of a novel human phosphatidic acid phosphatase type 2 isoform. *FEBS Lett.* **427**, 188–192
7. Brindley, D.N. and Waggoner, D.W. (1998) Mammalian lipid phosphate phosphohydrolases. *J. Biol. Chem.* **273**, 24281–24284
8. Zhang, N., Zhang, J., Purcell, K.J., Cheng, Y., and Howard, K. (1997) The *Drosophila* protein Wunen repels migrating germ cells. *Nature* **385**, 64–67
9. Starz-Gaiano, M., Cho, N.K., Forbes, A., and Lehmann, R. (2001) Spatially restricted activity of a *Drosophila* lipid phosphatase guides migrating germ cells. *Development* **128**, 983–991
10. Escalante-Alcalde, D., Hernandez, L., Le Stunff, H., Maeda, R., Lee, H.S., Jr Gang, C., Sciorra, V.A., Daar, I., Spiegel, S., Morris, A.J., and Stewart, C.L. (2003) The lipid phosphatase LPP3 regulates extra-embryonic vasculogenesis and axis patterning. *Development* **130**, 4623–4637
11. Kanoh, H., Kai, M., and Wada, I. (1997) Phosphatidic acid phosphatase from mammalian tissues: discovery of channel-like proteins with unexpected functions. *Biochim. Biophys. Acta* **1348**, 56–62
12. Kanoh, H., Kai, M., and Wada, I. (1999) Molecular characterization of the type 2 phosphatidic acid phosphatase. *Chem. Phys. Lipids* **98**, 119–126
13. Zhang, Q.X., Pilquil, C.S., Dewald, J., Berthiaume, L.G., and Brindley, D.N. (2000) Identification of structurally important domains of lipid phosphate phosphatase-1: implications for its sites of action. *Biochem. J.* **345**, 181–184
14. Jasinska, R., Zhang, Q.X., Pilquil, C., Singh, I., Xu, J., Dewald, J., Dillon, D.A., Berthiaume, L.G., Carman, G.M., Waggoner, D.W., and Brindley, D.N. (1999) Lipid phosphate phosphohydrolase-1 degrades exogenous glycerolipid and sphingolipid phosphate esters. *Biochem. J.* **340**, 677–686
15. Roberts, R., Sciorra, V.A., and Morris, A.J. (1998) Human type 2 phosphatidic acid phosphohydrolases. Substrate specificity

of the type 2a, 2b, and 2c enzymes and cell surface activity of the 2a isoform. *J. Biol. Chem.* **273**, 22059–22067
16. Ishikawa, T., Kai, M., Wada, I., and Kanoh, H. (2000) Cell surface activities of the human type 2b phosphatidic acid phosphatase. *J. Biochem.* **127**, 645–651
17. Miyamoto, S., Hirata, M., Yamazaki, A., Kageyama, T., Hasuwa, H., Mizushima, H., Tanaka, Y., Yagi, H., Sonoda, K., Kai, M., Kanoh, H., Nakano, H., and Mekada, E. (2004) Heparin-binding EGF-like growth factor is a promising target for ovarian cancer therapy. *Cancer Res.* **64**, 5720–5727
18. Tanyi, J.L., Hasegawa, Y., Lapushin, R., Morris, A.J., Wolf, J.K., Berchuck, A., Lu, K., Smith, D.I., Kalli, K., Hartmann, L.C., McCune, K., Fishman, D., Broaddus, R., Cheng, K.W., Atkinson, E.N., Yamal, J.M., Bast, R.C., Felix, E.A., Newman, R.A., and Mills, G.B. (2003) Role of decreased levels of lipid phosphate phosphatase-1 in accumulation of lysophosphatidic acid in ovarian cancer. *Clin. Cancer Res.* **9**, 3534–3545
19. Tanyi, J.L., Morris, A.J., Wolf, J.K., Fang, X., Hasegawa, Y., Lapushin, R., Auersperg, N., Sigal, Y.J., Newman, R.A., Felix, E.A., Atkinson, E.N., and Mills, G.B. (2003) The human lipid phosphate phosphatase-3 decreases the growth, survival, and tumorigenesis of ovarian cancer cells: validation of the lysophosphatidic acid signaling cascade as a target for therapy in ovarian cancer. *Cancer Res.* **63**, 1073–1082
20. Alderton, F., Darroch, P., Sambi, B., McKie, A., Ahmed, I.S., Pyne, N., and Pyne, S. (2001) G-protein-coupled receptor stimulation of the p42/p44 mitogen-activated protein kinase pathway is attenuated by lipid phosphate phosphatases 1, 1a, and 2 in human embryonic kidney 293 cells. *J. Biol. Chem.* **276**, 13452–13460
21. Hooks, S.B., Santos, W.L., Im, D.S., Heise, C.E., Macdonald, T.L., and Lynch, K.R. (2001) Lysophosphatidic acid-induced mitogenesis is regulated by lipid phosphate phosphatases and is Edg-receptor independent. *J. Biol. Chem.* **276**, 4611–4621
22. Sciorra, V.A. and Morris, A.J. (1999) Sequential actions of phospholipase D and phosphatidic acid phosphohydrolase 2b generate diglyceride in mammalian cells. *Mol. Biol. Cell* **10**, 3863–3876
23. Burnett, C. and Howard, K. (2003) Fly and mammalian lipid phosphate phosphatase isoforms differ in activity both in vitro and in vivo. *EMBO Rep.* **4**, 793–799
24. Nanjundan, M. and Possmayer, F. (2001) Pulmonary lipid phosphate phosphohydrolase in plasma membrane signalling platforms. *Biochem. J.* **358**, 637–646
25. Jia, Y.J., Kai, M., Wada, I., Sakane, F., and Kanoh, H. (2003) Differential localization of lipid phosphate phosphatases 1 and 3 to cell surface subdomains in polarized MDCK cells. *FEBS Lett.* **552**, 240–246
26. Ikonen, E. (2001) Roles of lipid rafts in membrane transport. *Curr. Opin. Cell Biol.* **13**, 470–477
27. Simons, K. and Ikonen, E. (1997) Functional rafts in cell membranes. *Nature* **387**, 569–572
28. Simons, K. and Toomre, D. (2000) Lipid rafts and signal transduction. *Nat. Rev. Mol. Cell Biol.* **1**, 31–39
29. Madore, N., Smith, K.L., Graham, C.H., Jen, A., Brady, K., Hall, S., and Morris, R. (1999) Functionally different GPI proteins are organized in different domains on the neuronal surface. *EMBO J.* **18**, 6917–6926
30. Roper, K., Corbeil, D., and Huttner, W.B. (2000) Retention of prominin in microvilli reveals distinct cholesterol-based lipid micro-domains in the apical plasma membrane. *Nat. Cell Biol.* **2**, 582–592
31. Ulrix, W., Swinnen, J.V., Heyns, W., and Verhoeven, G. (1998) Identification of the phosphatidic acid phosphatase type 2a isozyme as an androgen-regulated gene in the human prostatic adenocarcinoma cell line LNCaP. *J. Biol. Chem.* **273**, 4660–4665
32. Akagi, T., Shishido, T., Murata, K., and Hanafusa, H. (2000) v-Crk activates the phosphoinositide 3-kinase/AKT pathway in transformation. *Proc. Natl. Acad. Sci. USA* **97**, 7290–7295
33. Nagaya, H., Wada, I., Jia, Y.J., and Kanoh, H. (2002) Diacylglycerol kinase δ suppresses ER-to-Golgi traffic via its SAM and PH domains. *Mol. Biol. Cell* **13**, 302–316
34. Fukuda, M. (1985) Cell surface glycoconjugates as onco-differentiation markers in hematopoietic cells. *Biochim. Biophys. Acta* **780**, 119–150
35. Brown, D.A., and London, E. (1998) Functions of lipid rafts in biological membranes. *Annu. Rev. Cell Dev. Biol.* **14**, 111–136
36. Brown, D.A. and Rose, J.K. (1992) Sorting of GPI-anchored proteins to glycolipid-enriched membrane subdomains during transport to the apical cell surface. *Cell* **68**, 533–544
37. Sargiacomo, M., Sudol, M., Tang, Z., and Lisanti, M.P. (1993) Signal transducing molecules and glycosyl-phosphatidylinositol-linked proteins form a caveolin-rich insoluble complex in MDCK cells. *J. Cell Biol.* **122**, 789–807
38. Kunimoto, M., Shibata, K., and Miura, T. (1989) Comparison of the cytoskeleton fractions of rat red blood cells prepared with non-ionic detergents. *J. Biochem.* **105**, 190–195
39. Ojakian, G.K. and Schwimmer, R. (1988) The polarized distribution of an apical cell surface glycoprotein is maintained by interactions with the cytoskeleton of Madin-Darby canine kidney cells. *J. Cell Biol.* **107**, 2377–2387
40. Klein, U., Gimpl, G., and Fahrenholz, F. (1995) Alteration of the myometrial plasma membrane cholesterol content with β-cyclodextrin modulates the binding affinity of the oxytocin receptor. *Biochemistry* **34**, 13784–13793
41. Scheiffele, P., Roth, M.G., and Simons, K. (1997) Interaction of influenza virus haemagglutinin with sphingolipid-cholesterol membrane domains via its transmembrane domain. *EMBO J.* **16**, 5501–5508
42. Harder, T., Scheiffele, P., Verkade, P., and Simons, K. (1998) Lipid domain structure of the plasma membrane revealed by patching of membrane components. *J. Cell Biol.* **141**, 929–942
43. Rodriguez-Boulan, E., Kreitzer, G., and Musch, A. (2005) Organization of vesicular trafficking in epithelia. *Nat. Rev. Mol. Cell Biol.* **6**, 233–247
44. Humtsoe, J.O., Feng, S., Thakker, G.D., Yang, J., Hong, J., and Wary, K.K. (2003) Regulation of cell-cell interactions by phosphatidic acid phosphatase 2b/VCIP. *EMBO J.* **22**, 1539–1554